International Journal of Pharmaceutics 534 (2017) 308–315

Contents lists available at ScienceDirect

International Journal of Pharmaceutics

journal homepage: www.elsevier.com/locate/ijpharm

# An optimized two-vial formulation lipid nanoemulsion of paclitaxel for targeted delivery to tumor

Lina Chen[a,1], Bingchen Chen[b,1], Li Deng[a,1], Baoan Gao[a,c], Yuansheng Zhang[d], Chan Wu[a], Nong Yu[d], Qinqin Zhou[c], Jianzhong Yao[a,*], Jianming Chen[a,c,d,*]

[a] School of Pharmacy, Second Military Medical University, Shanghai 200433,China
[b] 6th Team of Student Brigade, Second Military Medical University, Shanghai 200433,China
[c] Jiangsu Tasly Diyi Pharmaceutical Co., Ltd, Jiangsu 223002, China
[d] Department of Pharmacy, Fujian University of Traditional Chinese Medicine, Fujian 350108, China

ARTICLE INFO

*Kewords:*
Paclitaxel
Two-vial formulation
Lipid nanoemulsion
Anticancer
MCF-7 cell

ABSTRACT

The discovery of new intravenous drug delivery carrier for water-insoluble drug is a challenging task. In this paper, novel two-vial formulation of paclitaxel (PTX)-loaded lipid nanoemulsions (TPLEs) with particle sizes of 110 nm (TPLE-1), 220 nm (TPLE-2) and 380 nm (TPLE-3), which were formed by mixing a PEG400 solution of PTX and 10% (*w/w*) blank lipid emulsions (BLEs) with different particle size prior to use, were developed and comparatively evaluated for their pharmaceutics, pharmacokinetics, biodistribution, in vitro and in vivo anticancer efficiency. Among them, TPLE-1 displayed higher PTX-loading, slower PTX-release and larger PTX-distribution in oil-phase, significantly reduced extraction by RES organs, increased tumor-uptake, showed stronger cytotoxicity against MCF-7 cells and more potent anticancer efficacy on MCF-7 tumor-bearing nude mice, and had greater plasma $AUC_{0-\infty}$ value, smaller plasma clearance (CL), longer mean residence time (MRT) and elimination half-life ($T_{1/2}$) in SD rats. It also exhibited the same in vivo efficacy as Taxol® and even produced less hemolysis and intravenous irritation. Moreover, its $LD_{50}$ was 4.3-fold higher than that of Taxol®. All results demonstrate that TPLE-1 is a promising candidate drug due to its high tumor-accumulation and effectiveness, low toxicity, good safety and druggability in clinical application for the cancer therapy.

## 1. Introduction

With development of drug discovery technology, more and more new active compounds come forward, and more than 60% of which are insoluble in water (Lipinski, 2000).[1] The clinical efficacy of these drugs is seriously reduced even though they have good pharmacological activity because of their defects such as low water solubility, low oral bioavailability, difficult to realize the diversification of forms and so on. To overcome these problems, water-insoluble drug delivery system for intravenous administration has become a hot point of research in the world (Kesisoglou et al., 2007; Alexis et al., 2010).

Lipid nanoemulsion, one of novel nanocarriers, has received more and more attention owing to its biocompatibility and ability to incorporate poorly water-soluble drugs (Tamilvanan, 2004). As an insoluble drug delivery medium for intravenous administration, it has some unique advantages. For example, it can reduce drug toxicity and intravenous irritation on the blood vessel, and increase drug tolerance, and improve therapeutic efficacy due to its passive targeting (Hippalgaonkar et al., 2010; Sarker, 2005; Kelmann et al., 2008; Seki et al., 2004).

The conventional drug-loaded lipid nanoemulsion was usually prepared by high pressure homogenisation after oil phase containing drugs was dispersed in water phase through phospholipids (Takegami et al., 2008; Benita and Levy, 1993; Keck and Müller, 2006; Suttmann et al., 1989; Jeppsson and Ljungberg, 1975; von Dardel et al., 1983). Müller also invented a SolEmuls® technology (Müller et al., 2004), which was generally accepted in the world (Akkar and Müller, 2003a, 2003b; Akkar et al., 2004). However, these direct drug-load methods had several disadvantages such as poor permanent storage stability, easy crystallization and complicated preparation process (Mishra et al., 2009; Krause et al., 2000).

In our previous work, we had invented a novel polyethylene glycol 400 (PEG400) mediated two-vial formulation of intravenous injectable lipid nanoemulsion as drug delivery carrier for poorly water-soluble drugs using paclitaxel (PTX) as model drug (Jing et al., 2014). The formulation consisted of a PEG400 solution of the drug and a

* Corresponding authors at: School of Pharmacy, Second Military Medical University, Shanghai 200433,China
*E-mail addresses:* yaojz6601@sina.com (J. Yao), yjcjm@163.com (J. Chen).
[1] These three authors contributed equally to this work.

http://dx.doi.org/10.1016/j.ijpharm.2017.10.005
Received 22 March 2017; Received in revised form 15 September 2017; Accepted 1 October 2017
Available online 03 October 2017
0378-5173/ 

commercially available 20% (*w/v*) injectable blank lipid emulsion (BLE), respectively. The drug solution and 20% (*w/v*) BLE were expediently mixed to form drug-loaded lipid nanoemulsion prior to use. Compared to conventional directly PTX-loaded lipid emulsion (CPLE), this two-vial formulation of PTX-loaded lipid nanoemulsion (TPLE) had some prominent advantages such as high drug-loading rate, susceptible to escape the phagocytosis by reticuloendothelial system (RES) organs, low toxicity to RES organs, excellent permanent storage stability (≥24 months), etc. However, it regrettably exhibited less anti-cancer efficacy in vivo than Taxol® (data not shown).

Considering that the particle size has usually distinct effects on biodistribution, drug-release and in vivo efficacy (Seki et al., 2004; Takino et al., 1994; Fukui et al., 2003), we intend to further optimize the formulation and the particle size of original TPLE in order to improve its anticancer efficacy. In this paper, a novel TPLEs with particle sizes of 110 nm (TPLE-1), 220 nm (TPLE-2) and 380 nm (TPLE-3), which are handily formed by mixing a PEG400 solution of PTX and 10% (*w/w*) injectable BLEs with the corresponding particle size prior to use, are well designed and prepared. Their drug-loading capacity, drug-release, phase distribution, pharmacokinetics, biodistribution, cytotoxicity against MCF-7 cells and anticancer efficacy on MCF-7 tumor-bearing nude mice are comparatively evaluated. Furthermore, acute toxicity and intravenously injection safety (including irritation and hemolysis) for the most effective are also assessed.

## 2. Materials and methods

### 2.1. Chemicals

PTX and docetaxel (DTX) (Meilian Pharma Ltd., Chongqing, China), PL-100 M (Japanese kewpie company, Japan), long chain oil (LCT) and medium chain oil (MCT) (Tieling Beiya Medicinal Oil Co. Ltd., Liaoning, China), glycerol (Shantou Ziguang Guhan Amino Acid Co. Ltd., Shantou, China), PEG400, isopropanol and ethanol (Sinopharm Chemical Reagent Ltd., Shanghai, China), oleic acid (Lipoid GmbH, Ludwigshafen, Germany), Tween-80 (ICN Biomedical Inc., OH, USA), Dulbeccro's modified Eagle's medium (DMEM) and 10% fetal bovine serum (FBS) (Gibco Laboratories, NY, USA), Cell Counting Kit-8 (CCK-8) (Dojindo Laboratories Co., Kumamoto, Japan), acetonitrile, methanol, formic acid, dimethyl sulphoxide (DMSO) (Merck, Darmstadt, Germany). All other chemicals and solvents used were of analytical or pharmaceutical grade.

### 2.2. Cells and animals

Human breast cancer MCF-7 cells (Cell Culture Center of the Shanghai Institutes for Biological Sciences of the China Academy of Sciences, Shanghai, China). MCF-7 cells were preserved in cell cryoprotectant which contained 15% FBS, 8% DMSO and 77% DMEM in liquid nitrogen. The frozen cells were to unfreeze quickly at 38 °C in water followed by centrifuging at 1000 rpm for 2–3 min. After removing the cell cryoprotectant, the cells were grown in tissue culture flasks in complete growth medium (DMEM medium supplemented with 10% FBS, 100 mg/mL streptomycin and 100 units/mL penicillin) in carbon dioxide incubator at 37 °C, 5% $CO_2$ and 98% relative humidity (RH).

Sprague-dawley (SD) rats, ICR mice, BALB/c-Nu mice and New Zealand white rabbits (Shanghai SLAC Laboratory Animal Co. Ltd., Shanghai, China). Female nude mice were housed in a pathogen-free environment at 5–6 mice per cage. The animals were acclimatized for 4–7 days before experimentation, fed with standard diet and allowed water adlibitum. All animal experiments were performed in accordance with guidelines approved by the ethics committee of Second Military Medical University.

### 2.3. Pharmaceutical studies

#### 2.3.1. Preparation of TPLEs

MCT-LCT (1:1, *w/w*) (10.0 g) and oleic acid (30 mg) were mixed as the oil phase. Glycerol (2.2 g), PL–100 M (1.2 g) and distilled $H_2O$ (86.57 g) were mixed as the aqueous phase. The oil phase was added slowly into the aqueous phase with high speed shear apparatus (JRJ-300-1, Shanghai, China) for 15 min to form the coarse emulsion at 75–80 °C. The coarse emulsion was passed through a high pressure homogenizer (M-110EH, Newton, MA, USA) for one cycle at the pressure of 4000 psi and 10000 psi to produce 10% (*w/w*) blank lipid nanoemulsions (BLEs) with particle size of 380 nm (BLE-3) and 220 nm (BLE-2), respectively. The BLE with particle size of 110 nm (BLE-1) also was obtained by homogenizing at the pressure of 20000 psi for 15 cycles. Then BLEs were packaged after nitrogen purging and sterilized at 121 °C for 15 min. A definite quantity of PTX ranged from 42 mg to 300 mg was dissolved in 4 mL of PEG400 and the solution was sterilized at 121 °C for 15 min after it was adjusted to pH 3.0 by citric acid. Then 4 mL of PTX-PEG400 solution was directly injected to 96 mL of sterile BLEs (BLE-1, BLE-2 and BLE-3) to form a certain concentration of PTX-loaded emulsion while handily shaked for 1–2 min to make it uniform dispersion, including TPLE-1, TPLE-2, and TPLE-3. At meanwhile, 4 mL of PEG400 was mixed with 96 mL of sterile BLEs to form blank TPLEs according to above method.

#### 2.3.2. Physical stability studies

In order to study the drug-loading capacity of TPLEs with different particle size, the different concentrations of TPLE-1, TPLE-2 and TPLE-3 were freshly prepared and their stabilities were investigated at appropriate time intervals at 25 °C ( ± 2 °C)/RH 60% ( ± 5%). The stability parameters including drug content and particle size were determined as the functions of stability time. Furthermore, the particle size and zeta potential of BLEs, Blank TPLEs and TPLEs with good stability (*i.e.* PTX content ≥98%) at minimum and maximum concentrations were also examined. The particle diameter and zeta potential were determined by Malvern Zetasizer (Nano ZS 90, UK). As PTX in TPLEs could be gradually precipitated crystals, TPLEs at different time intervals would be filtered through 0.22 μm membrane filter (Pall Corp., East Hills, NY, USA). The subsequent filtrates were diluted with isopropanol and the quantification of PTX in the resulting sample was performed by HPLC analysis. Results were expressed as mean ± SD ($n$ = 3).

#### 2.3.3. in vitro drug release

In vitro releases of PTX from different sizes of TPLEs with the same concentration (0.7 mg/mL) were carried out in a Pharmaceutical Dissolution Tester (Rcz-6c2, Shanghai, China) by basket-rotating method. 1 mL of TPLEs was instilled into the dialysis bags (MWCO: 12000, Spectrum Medical Industries Inc., Houston, USA). The bags were firmly sealed and then placed in 250 mL of PBS containing 1.5% (*w/v*) Tween-80. The basket revolution speed was 100 rpm and the temperature was (37 ± 1) °C. At the pre-determined time intervals (0, 0.5, 1, 2, 4, 6, 8, 10, 12 h), 4 mL of sample was taken out and an equal volume of fresh release medium was replenished. The samples at different time points were filtered through 0.45 μm membrane and analyzed by HPLC.

#### 2.3.4. Phase distribution assessment

The drug distribution in lipid emulsion was estimated according to the literature (Sila-on et al., 2008). Appropriate amount of TPLEs (0.70 mg/mL) were ultracentrifuged at 22000 rpm for 4 h at room temperature. Then the emulsions were divided into 3 layers, which were oil phase, phospholipids layer and aqueous phase from top to bottom, respectively. The oil phase was diluted with isopropanol to an appropriate concentration for HPLC analysis. The aqueous phase was filtered through 0.45 μm filter membrane and the subsequent filtrate was collected for HPLC analysis. The PTX content in phospholipids

layer was obtained by the total PTX content in TPLEs minus the content of PTX in oil phase and aqueous phase.

### 2.4. in vitro cytotoxicity assay

The cytotoxicity of samples was evaluated by the CCK-8 assay (Mao et al., 2013; Zhu et al., 2012). Briefly, MCF-7 cells in logartithmic growth phase were added to 96-well plates at a density of $3 \times 10^3$ cells per well. The cells were incubated at 37 °C over night in 5% $CO_2$ atmosphere (Thermo, USA). Then various concentrations of TPLEs and Taxol® (0.05, 0.11, 0.23, 0.50, 1.07, 2.30, 4.94 μg/mL) were respectively added to each well and every concentration was set to 5 repeated well. After 48 h incubation, 10 μL cell counting Kit-8 (CCK-8) solution was added to each well and sequentially incubated for 2 h, and then the absorption value at 490 nm was measured on a microplate reader (MK-3, Thermo, USA) followed to calculate the cell inhibition rate while the reference wavelength was set to 650 nm. Each assay was repeated three times. Taxol® was set as positive control, PBS and blank TPLE-1 being set as negative control.

### 2.5. Biological studies

#### 2.5.1. Pharmacokinetics study

18 male SD rats weighing 180–220 g were randomly divided into three groups and intravenously administered with TPLE-1, TPLE-2 and TPLE-3 (each 1 mg/mL) at a same dosage of 15 mg/kg, respectively. The blood samples (0.5 mL) were collected from the retro-orbital plexus into heparinized microcentrifuge tubes (containing heparin) at appropriate time intervals (2, 5, 10, 20, 40 min and 1, 2, 3, 4, 6, 8 h) and centrifuged at 3500 rpm for 10 min to isolate the plasma samples (Shaikh et al., 2009). Pharmacokinetic (PK) parameters were calculated by Kinetica 4.4 Software based on two compartment model.

#### 2.5.2. Biodistribution study

72 female BALB/c-Nu mice bearing MCF-7 tumor weighing 18–20 g were randomly divided into three groups and received TPLE-1, TPLE-2 and TPLE-3 (each 1 mg/mL) at a same dosage of 15 mg/kg via the tail vein, respectively. At the predetermined time points (5 min and 0.25, 0.5, 1, 2, 3, 7, 12 h), 3 mice were taken out and the blood samples were collected from the retro-orbital sinus into heparin treated tubes. Then, the mice were euthanized by cervical dislocation and the tissues including tumor, liver, kidney, heart, spleen, and lungs were collected. The blood was centrifuged at 3500 rpm for 10 min to isolate the plasma (Ganta et al., 2008). 0.1 g of tissue was homogenized with 0.3 mL of saline to get tissues sample.

#### 2.5.3. PTX extraction

To determine PTX content, 20 μL of DTX (40 μg/mL) as interior standard and 1.5 mL of methyl *tert*-butyl ether (MTBE) were added into 200 μL of above plasma or tissue samples. After vortexing for 5 min with the vortex-5 mixer (Haimen its BEI'ER Instrument Manufacturing Co Ltd), the samples were centrifuged at 8000 rpm for 15 min to make the impurities precipitate. Then the organic layer was collected and combined after repeating the above extraction procedure, and then dried in vacuum. The residues were reconstituted with 200 μL of methanol for HPLC analysis (Li and Choi, 2007; Ma et al., 2013).

#### 2.5.4. Antitumor efficacy

The antitumor efficacy was evaluated in BALB/c-Nu mice (4–5 weeks of age, female, 16–20 g). Mice were subcutaneously inoculated with MCF-7 breast cancer cells ($1 \times 10^7$ cells/0.2 mL). When the tumor grew to 70–120 $mm^3$ in volume (Yao et al., 2011; Lee et al., 2011), mice were randomly divided into 6 groups including saline, blank TPLE-1, TPLE-1, TPLE-2, TPLE-3 and Taxol® group, each group of 6 mice. Blank TPLE-1 and saline were set as negative controls, Taxol® being set as positive control. TPLE-1, TPLE-2 and TPLE-3 (each 1 mg/mL) were individually administered intravenously at a same dosage of 15 mg/kg through the tail vein. Mice were administered with tested drug for three times on day 0, 3 and 6. Tumor size and body weight of the mice were measured on day 2, 4, 6, 7, 9 for antitumor efficacy and safety evaluation. The animals were sacrificed by cervical dislocation on day 9 and the tumor mass was harvested and weighted. Individual tumor volumes (V) were calculated by the formula: $V = [L \times W^2]/2$, where length (L) was the longest diameter and width (W) was the shortest diameter perpendicular to length. Tumor growth curves were presented as the mean volume relative to the values on the first day of the treatment. The relative tumor growth rate (RTV, %) was calculated by the formula: $RTV = [(V_t/V_0)/(V_{ct}/V_{c0})] \times 100\%$, where $V_t$ and $V_0$ were the mean tumor volumes of test group on day 9 and day 0, respectively while $V_{ct}$ and $V_{c0}$ were the mean tumor volumes of the blank TPLE-1 group on day 9 and day 0, respectively. The tumor inhibitory rate (TIR) was calculated by the following formula: $TIR = [(TW_0–TW_1)/TW_0] \times 100\%$, where $TW_0$ and $TW_1$ were the mean tumor weight for blank TPLE-1 and test drug groups, respectively.

### 2.6. Intravenous injection safety assessment

#### 2.6.1. Intravenous irritation assessment

Two rabbits weighting 2.0–2.5 kg were respectively injected with a daily dosage of 6.0 mg/kg of TPLE-1 and Taxol® at the concentration of 2.0 mg/mL into the right ear vein at an injection rate of 1.0 mL/min for 3 days, and an equivalent volume of saline was injected into the left ear vein meanwhile as control. The rabbits were sacrificed by bloodletting at 48 h after the last administration, and then a piece of vascular tissue at the injection site was cut, fixed in 4% paraformaldehyde and embedded with paraffin for histopathological examination (Zhang et al., 2008).

#### 2.6.2. Hemolysis test

Rabbit blood (10 mL) was collect in 100 mL conical flask containing glass pearls. The fibrinogen was removed by shaking softly for 10 min. The erythrocytes were washed with 5% glucose injection for several times until the supernatant was clear. Then the erythrocytes were dispersed in 5% glucose injection to give 2% suspension. 5% glucose injection (2.5 mL), water (2.5 mL), different volumes (2.0, 1.6, 1.2 mL) of Taxol® (2 mg/mL) and different volumes (2.0, 1.8, 1.6, 1.4, 1.2 mL) of TPLE-1 (2 mg/mL) were added into ten tubes with 2.5 mL of 2% erythrocyte suspension in each, respectively. Their final volumes were all regulated with 5% glucose injection to 5 mL 5% Glucose injection was used as negative control, water and Taxol® used as positive control. After vortex, the tubes were incubated for 3 h at 37 °C and stayed for 5 min at 0 °C. Hemolysis of TPLE-1 was evaluated by visual observation (Zhang et al., 2008).

#### 2.6.3. Acute toxicity

130 ICR mice (half male and half female, 18–22 g) were randomly divided into 13 groups: six TPLE-1-treated groups at dosages of 61, 87, 124, 176, 250 and 356 mg/kg, respectively; seven taxol-treated groups at dosages of 20, 30, 43, 60, 88, 126 and 180 mg/kg, respectively. Each group contained 10 mice and the mice were injected with various dosages of TPLE-1 or Taxol® via the tail vain once. The mice were observed every day for 2 weeks after drug administration and the number of death was recorded (Gao et al., 2013). Then the $LD_{50}$ value was calculated by the Bliss method.

### 2.7. HPLC assay

A reversed-phase Agilent HPLC 1100 (Agilent Corporation, American) was used for the determination of paclitaxel. DTX was used as an internal standard. The mobile phase consisting of acetonitrile and double-distilled water (55:45, *v/v*) was pumped through the Ultimate XB-C18 column (250 × 4.6 mm, particle size: 5 μm, Ultimate

Corporation, USA). The elution was carried out at a flow rate of 1.0 mL/min, and the column temperature was maintained at 30 °C. 20 μL of the samples were analyzed at the wavelength of 227 nm with ultraviolet-visible detector (G1314BUV-vis). Chromatograms of blank plasma and plasma spiked with PTX and DTX were shown in Supplementary material. The peaks of PTX and DTX were distinctly separated; the retention times of PTX and DTX were 10.4 and 12.4 min, respectively. The detection limit of PTX was 28 ng/mL. The coefficient of variation for intra-run and inter-run of PTX was below 3.68% and 3.53%, respectively (see Supplementary material).

### 2.8. Statistical analysis

Results were expressed as mean ± standard deviation (SD) and software SPPS PASW Statistic 18.0 was used for evaluation of statistical significance.

## 3. Results

### 3.1. Physical stability of TPLE-1, TPLE-2 and TPLE-3

Below 2% of PTX loss in 12 h was defined as the critical index for physical stability of TPLEs. As shown in Supplementary material, the maximum drug-loaded rates of TPLE-1, TPLE-2 and TPLE-3 were respectively 2.3 mg/mL, 1.3 mg/mL and 0.7 mg/mL, indicating that PTX-loaded rate in TPLEs increased as the particle size decreased. In addition, there is no change in particle size between BLEs and corresponding TPLEs or blank TPLEs. Moreover, the Zeta potentials of BLEs, blank TPLEs and TPLEs with good stability (PTX content ≥ 98%) at minimum and maximum drug-loaded concentrations in different time intervals had no statistical difference, suggesting that the zeta potential wasn't correlated with particle diameter in the range from 110 nm to 380 nm (Table 1).

### 3.2. in vitro drug release

The terminal time point of PTX-release test was selected as 12 h because TPLEs (each 0.7 mg/mL) could be stable within 12 h. As shown in Fig. 1, all TPLEs exhibited a biphasic pattern characterized by a fast PTX release during the initial 4 h and a subsequent sustained PTX release. At the determined time intervals, PTX from TPLE-1 was released slower than that from TPLE-2 or TPLE-3. The accumulated release percentage of PTX at 12 h was 51.67% ± 1.20% for TPLE-3, 39.96% ± 0.54% for TPLE-2, 33.08% ± 0.90% for TPLE-1, suggesting that in vitro PTX-release rate slowed down as the particle size decreased.

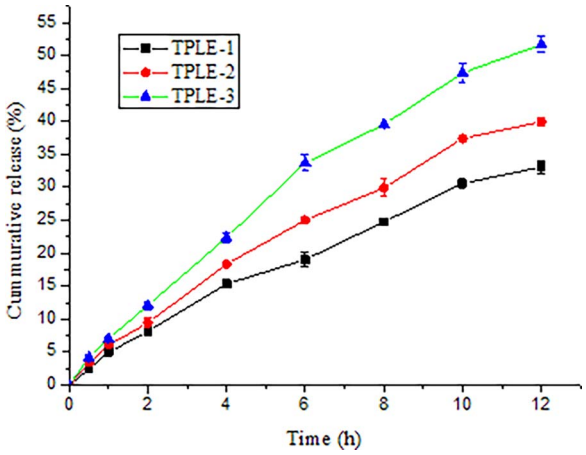


**Fig. 1.** Release kinetics of PTX from TPLEs under the concentration of 0.7 mg/mL at pH 7.4.

**Table 2**
Comparative phase distribution of PTX in TPLEs at a concentration of 0.7 mg/mL.

| TPLEs | MC[a] | DC[a] | PTX content (%) | | |
|---|---|---|---|---|---|
| | (mg/mL) | (mg/mL) | Oil | Water | Lipid |
| TPLE-1 | 0.70 | 0.71 | 39.25 ± 2.7* | 1.38 ± 0.5 | 59.36 ± 2.5* |
| TPLE-2 | 0.70 | 0.71 | 32.36 ± 2.0** | 1.67 ± 0.6 | 65.97 ± 1.6** |
| TPLE-3 | 0.70 | 0.68 | 25.71 ± 0.9*** | 1.32 ± 0.5 | 72.96 ± 1.1*** |

[a] Abbreviation: MC, Marked Concentration; DC, Determined Concentration. Data as mean ± SD ($n$ = 3).
* $P < 0.05$, when compared with TPLE-2.
** $P < 0.05$, when compared with TPLE-3.
*** $P < 0.01$, when compared with TPLE-1.

### 3.3. Phase distribution assessment

As shown in Table 2, majority of PTX in TPLEs was dispersed in phospholipids layer. The average percentage of PTX in oil phase was 39.25% ± 2.7% for TPLE-1, 32.36% ± 2.0% for TPLE-2 and 25.71% ± 0.9% for TPLE-3, indicating that TPLE-1 displayed a relative greater proportion of PTX in oil phase than TPLE-2 ($P < 0.05$) and TPLE-3 ($P < 0.01$). On the contrary, the average percentage of PTX in phospholipids layer was 59.36% ± 2.5% for TPLE-1, 65.97% ± 1.6% for TPLE-2 and 72.96% ± 1.1% for TPLE-3, suggesting that a relative smaller share of PTX in TPLE-1 was incorporated into phospholipids layer compared to TPLE-2 ($P < 0.05$) and TPLE-3 ($P < 0.01$). However, there was no statistical difference in percentage

**Table 1**
Time-course particle size and zeta potential of BLEs, blank TPLEs and TPLEs at different concentrations investigated at 25 °C ( ± 2 °C)/RH[a] 60% ( ± 5%).

| Samples | PTX (mg/mL) | 0 h | | 12 h | |
|---|---|---|---|---|---|
| | | particle size (nm) | zeta potential (mV) | particle size (nm) | zeta potential (mV) |
| BLE-1 | – | 112.3 ± 1.6 | −51.5 ± 2.2 | 112.7 ± 1.4 | −52.6 ± 2.4 |
| Blank TPLE-1 | – | 113.1 ± 2.1 | −52.9 ± 2.0 | 112.5 ± 1.9 | −54.7 ± 1.5 |
| TPLE-1 | 1.3 | 111.5 ± 1.6 | −55.1 ± 2.3 | 112.1 ± 1.3 | −55.3 ± 1.9 |
| TPLE-1 | 2.3 | 112.7 ± 1.8 | −54.4 ± 1.6 | 113.2 ± 1.7 | −53.2 ± 2.1 |
| BLE-2 | – | 225.1 ± 1.9 | −57.7 ± 2.2 | 224.6 ± 1.6 | −55.4 ± 2.0 |
| Blank BLE-2 | – | 223.0 ± 0.8 | −55.9 ± 1.8 | 223.8 ± 1.2 | −54.6 ± 1.9 |
| TPLE-2 | 0.5 | 226.2 ± 2.3 | −56.3 ± 1.5 | 225.4 ± 1.6 | −58.0 ± 1.7 |
| TPLE-2 | 1.3 | 225.8 ± 2.0 | −55.8 ± 2.3 | 226.6 ± 2.2 | −52.4 ± 2.3 |
| BLE-3 | – | 381.1 ± 3.7 | −53.5 ± 1.9 | 381.7 ± 3.4 | −54.5 ± 2.6 |
| Blank TPLE-3 | – | 382.5 ± 3.9 | −52.6 ± 2.1 | 383.1 ± 3.3 | −53.1 ± 2.0 |
| TPLE-3 | 0.5 | 383.3 ± 3.4 | −54.2 ± 1.6 | 383.6 ± 3.6 | −57.2 ± 2.5 |
| TPLE-3 | 0.7 | 383.7 ± 2.9 | −56.1 ± 2.4 | 383.1 ± 3.2 | −53.9 ± 2.1 |

Data as mean ± SD ($n$ = 3). [a] Abbreviation: RH, Relative humidity.

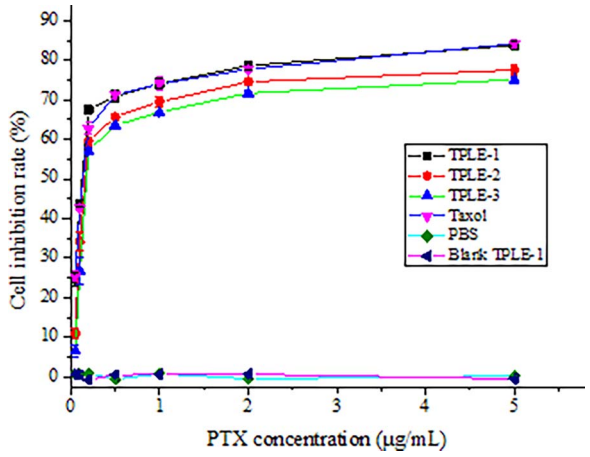


**Fig. 2.** Cytotoxicity of PBS, blank TPLE-1, TPLEs and Taxol against MCF-7 cells. Data as mean ± SD ($n$ = 3).

of PTX in aqueous phase between TPLEs ($P > 0.05$). The results showed that as the particle size in TPLEs decreased, PTX distribution in oil phase increased while it decreased in phospholipids layer.

### 3.4. in vitro cytotoxicity assay

The CCK-8 assay showed that there was significant difference in inhibition rate between TPLEs and Taxol® at different concentrations (0.05, 0.11, 0.23, 0.50, 1.07, 2.30, 4.94 μg/mL) against MCF-7 cells (Fig. 2). The $IC_{50}$ values were 0.158 ± 0.009 μg/mL for TPLE-1, 0.321 ± 0.018 μg/mL for TPLE-2 and 0.430 ± 0.021 μg/mL for TPLE-3 and 0.171 ± 0.011 for Taxol®, The difference of $IC_{50}$ value between TPLEs each other was statistically significant. However, there was no significant difference in $IC_{50}$ value between TPLE-1 and Taxol®. The results indicated that TPLE-1 exhibited stronger cytotoxicity than TPLE-2 ($P < 0.005$) or TPLE-3 ($P < 0.005$) and had the same cytotoxicity against MCF-7 cells as Taxol® ($P > 0.05$). In addition, there was no cytotoxicity on MCF-7 cells for the negative control groups.

### 3.5. Pharmacokinetics study

PTX concentration-time curves in plasma after intravenously administration of TPLEs in SD rats and the calculated pharmacokinetic parameters were shown in Fig. 3 and Table 3, respectively. The plasma $AUC_{0-\infty}$ value of TPLE-1 (23.09 ± 1.5 μg·h/mL) was approximately 1.6- and 2.5-fold greater than that of TPLE-2 (13.81 ± 1.0 μg·h/mL)

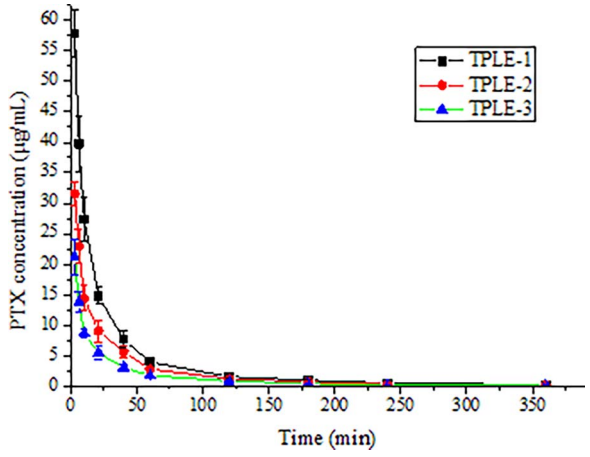


**Fig. 3.** Plasma concentration-time curves for PTX after intravenous administration of TPLEs in SD rats at a dosage of 15 mg/kg. Data as mean ± SD ($n$ = 6).

**Table 3**
Pharmacokinetic parameters after intravenous administration of TPLEs at a dose of 15 mg/kg.

| TPLEs | $AUC_{0-\infty}$ (μg h/mL) | CL (L/h) | $T_{1/2}$ (h) | MRT (h) |
|---|---|---|---|---|
| TPLE-1 | 22.08 ± 1.55$^{***}$ | 0.47 ± 0.07 | 1.50 ± 0.12 | 0.99 ± 0.07 |
| TPLE-2 | 14.14 ± 1.03$^{\Delta\Delta\Delta}$ | 0.52 ± 0.04$^{\Delta\Delta}$ | 1.34 ± 0.10$^{\Delta\Delta}$ | 0.94 ± 0.07$^{\Delta}$ |
| TPLE-3 | 8.17 ± 0.67$^{*}$ | 0.65 ± 0.07$^{*}$ | 1.07 ± 0.11$^{*}$ | 0.84 ± 0.06$^{*}$ |

Data as mean ± SD ($n$ = 6).
$^{***}P < 0.001$, when compared with TPLE-2
$^{\Delta}P < 0.05$.$^{\Delta\Delta}P < 0.01$.$^{\Delta\Delta\Delta}P < 0.001$, when compared with TPLE-3
$^{*}P < 0.01$, when compared with TPLE-1.

and TPLE-3 (8.17 ± 0.7 μg·h/mL), respectively. The mean residence time (MRT) for TPLE-1 (0.99 ± 0.07 h) ($P < 0.001$) and TPLE-2 (0.94 ± 0.07 h) ($P < 0.05$) was both significantly higher than that for TPLE-3 (0.84 ± 0.06 h). The elimination half-life ($T_{1/2}$) for TPLE-1 (1.50 ± 0.12 h) ($P < 0.001$) and TPLE-2 (1.34 ± 0.10 h) ($P < 0.01$) was all longer than that for TPLE-3 (1.06 ± 0.10 h). The plasma clearance (CL) for TPLE-1 (0.47 ± 0.07 L/h) ($P < 0.001$) and TPLE-2 (0.52 ± 0.04 L/h) ($P < 0.01$) was both shorter than that for TPLE-3 (0.65 ± 0.06 L/h). However, there was no statistically difference in MRT, $T_{1/2}$ or CL between TPLE-1 and TPLE-2.

### 3.6. Biodistribution study

The time-dependent *in vivo* biodistribution of PTX after intravenously administration of TPLEs in BALB/c-Nu mice bearing MCF-7 tumors and the calculated $AUC_{0-\infty}$ values of plasma and tissues were shown in Fig. 4 and in Table 4, respectively.

TPLEs were all extracted instantly in liver, reaching a highest concentration of PTX at equivalent doses of PTX (15 mg/kg) (Fig. 4A and B). As shown in Table 4, $AUC_{liver}$, $AUC_{spleen}$ and $AUC_{lung}$ values of TPLE-1 were all significantly lower than those of TPLE-2 ($P < 0.01$, $P < 0.05$ and $P < 0.05$) and TPLE-3 ($P < 0.001$, $P < 0.01$ and $P < 0.01$), respectively. In addition, $AUC_{liver}$ and $AUC_{spleen}$ values of TPLE-2 were also significantly lower than those of TPLE-3 ($P < 0.05$), respectively. These results suggested that extraction of PTX by RES organs (liver, spleen and lung) decreased as particle sizes of TPLEs decreased. As a result, TPLE-1 could effectively reduce extraction of RES organs compared to TPLE-2 and TPLE-3.

Importantly, the intratumor PTX content between TPLEs already displayed obvious difference at 0.5 h, which reached to the highest in 1 h. (Fig. 4C). The highest PTX concentration at 1 h was 4.91 ± 0.32 μg/g for TPLE-1, 3.37 ± 0.31 μg/g for TPLE-2 and 2.86 ± 0.18 μg/g for TPLE-3, and there was significant difference between TPLE-1 and other TPLEs ($P < 0.001$). Furthermore, $AUC_{tumor}$ value of TPLE-1 was significantly higher than that of TPLE-2 ($P < 0.01$) and TPLE-3 ($P < 0.001$). Moreover, $AUC_{tumor}$ value of TPLE-2 was also significantly higher than that of TPLE-3 ($P < 0.05$). These results indicated that uptake of PTX by tumor tissues increased as particle sizes of TPLEs decreased, and TPLE-1 could quickly target to the tumor tissues with a relatively higher concentration compared to TPLE-2 and TPLE-3.

Additionally, PTX concentration of TPLE-1 in plasma is higher than that of TPLE-2 and TPLE-3 (Fig. 4D), and there was significant difference in $AUC_{plasma}$ value between TPLEs each other ($P < 0.05$ or $P < 0.01$). PTX distributions in heart and kidney had no significant differences between TPLEs each other.

### 3.7. Antitumor efficacy

Table 5 displayed the inhibition profiles of TPLEs in MCF-7 breast tumor model at experimental last day. Fig. 5 illustrated the antitumor efficacy and safety of TPLEs at throughout period of experiment.

As shown in Fig. 5 and Table 5, TPLEs all could inhibit the tumor

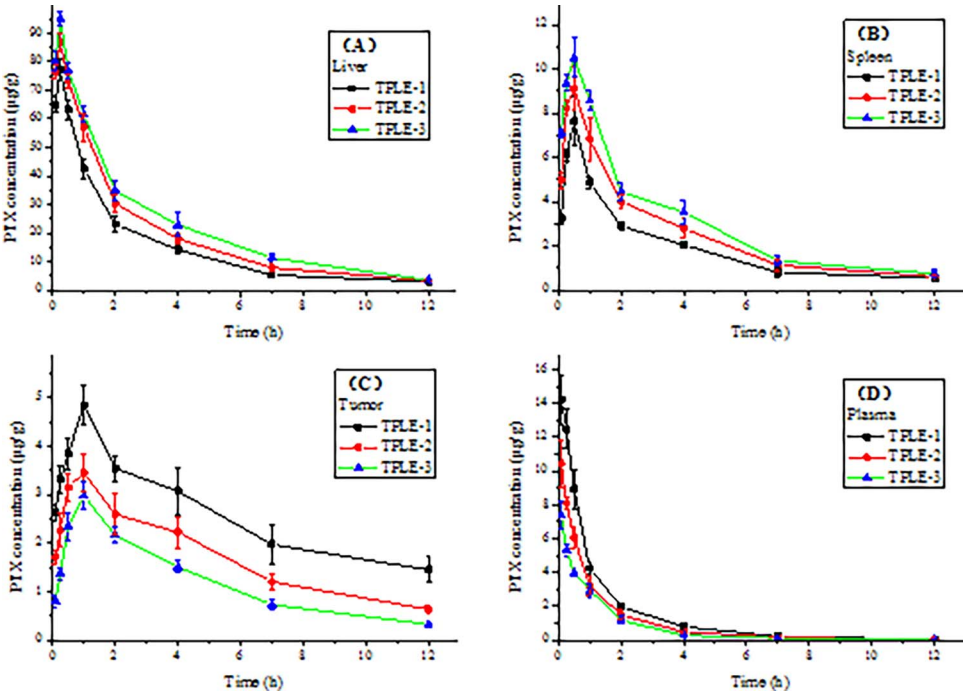


**Fig. 4.** Time-course profiles of PTX levels in tissues of MCF-7 tumor-bearing nude mice after intravenous administration of TPLEs at a dosage of 15 mg/kg. Data as mean ± SD ($n$ = 3).

**Table 4**
$AUC_{0-\infty}$ values of PTX in plasma and tissues after intravenous administration of TPLEs at a dose of 15 mg/kg.

| Tissues | AUC(μg h/g) | | |
|---|---|---|---|
| | TPLE-1 | TPLE-2 | TPLE-3 |
| Heart | 27.44 ± 1.5 | 26.07 ± 3.0 | 25.78 ± 3.9 |
| Liver | 176.68 ± 12.2$^{**}$ | 225.16 ± 15.3$^{\Delta,}$ | 264.10 ± 13.6$^{****}$ |
| Spleen | 21.88 ± 1.3$^{*}$ | 29.39 ± 1.8$^{\Delta}$ | 35.27 ± 3.7$^{***}$ |
| Lung | 26.07 ± 3.5$^{*}$ | 39.52 ± 6.5 | 43.49 ± 6.3$^{***}$ |
| Kidney | 37.30 ± 3.6 | 38.30 ± 2.9 | 37.67 ± 2.4 |
| Tumor | 30.44 ± 2.5$^{**}$ | 20.06 ± 2.7$^{\Delta}$ | 13.94 ± 0.9$^{****}$ |
| Plasma | 16.62 ± 1.9$^{**}$ | 11.74 ± 1.6$^{\Delta}$ | 8.46 ± 0.8$^{***}$ |

$^{*}P < 0.05$ and $^{**}P < 0.01$, when compared with TPLE-2; $^{\Delta}P < 0.05$, when compared with TPLE-3; $^{***}P < 0.01$ and $^{****}P < 0.001$, when compared with TPLE-1. Data as mean ± SD ($n$ = 3).

growth significantly compared to saline and blank TPLE-1 (Fig. 5B). In either tumor weight or tumor volume, there was significant difference between TPLEs each other, and but no significant difference between TPLE-1 and Taxol® ($P > 0.05$). Consequently, TPLE-1 showed greater TIR and smaller RTV than TPLE-2 and TPLE-3, and also had the same anticancer efficacy as Taxol®. Moreover, there was no appreciable decrease in body weight of TPLEs-treated mice (Fig. 5A). These results suggested that TPLE-1 exhibited low toxicity, and possessed the most potent antitumor efficacy among TPLEs, indicating that anticancer effect of TPLEs enhanced with the decreasing of the particle size.

### 3.8. Intravenous injection safety

#### 3.8.1. Intravenous irritation

There was no apparent histopathologic change in TPLE-1-treated group compared with saline group during the 3-day administration. In contrast, severe reddish discoloration, thrombus and tissue edema were observed in Taxol® group. These results indicated that TPLE-1 had no stimulative response on ear vein of rabbit at a dose of 6.0 mg/kg. Histopathology images were shown in Supplementary material.

#### 3.8.2. Hemolysis evaluation

Complete hemolysis could be observed in tubes of Taxol® and water at 15 min and no erythrocyte survived at the bottom of these tubes. The erythrocytes precipitated at the bottom of other six tubes of TPLE-1 and could disperse after shaking. These results demonstrated that TPLE-1 didn't cause haematolysis or agglutination reaction at 37 °C even in the PTX concentration of 0.8 mg/mL. However, Taxol® had produced complete hemolysis at PTX concentration of 0.48 mg/mL. The visual observation was shown in Supplementary material.

#### 3.8.3. Acute toxicity

The $LD_{50}$ of TPLE-1 administrated by intravenously injection was 259.5 mg/kg. The corresponding $LD_{50}$ of the Taxol® was 61.0 mg/kg, which was 4.3-fold lower than that of TPLE-1. This result demonstrated that TPLE-

**Table 5**
Tumor inhibition profiles of TPLEs in MCF-7 breast tumor mode after intravenous administration.

| Sample | Dose | $TV_0$ ($mm^3$) [a] | TW (g) [a] | $TV_1$ ($mm^3$) [a] | TIR (%) | RTV(%) |
|---|---|---|---|---|---|---|
| Saline | 15 mL/kg | 101.3 ± 11.43 | 1.51 ± 0.11 | 1587.3 ± 192.5 | | |
| Blank TPLE-1 | 15 mL/kg | 102.5 ± 12.80 | 1.60 ± 0.15 | 1607.2 ± 185.6 | | |
| TPLE-1 | 15 mg/kg | 103.4 ± 12.50 | 0.140 ± 0.03$^{*,\Delta\Delta\Delta}$ | 202.5 ± 35.6$^{*,\Delta\Delta}$ | 91.25 | 12.49 |
| TPLE-2 | 15 mg/kg | 101.5 ± 10.92 | 0.327 ± 0.05$^{*,***}$ | 355.3 ± 64.7$^{*,\ **}$ | 79.56 | 22.32 |
| TPLE-3 | 15 mg/kg | 100.8 ± 12.31 | 0.494 ± 0.07$^{*,\&\&\&}$ | 561.3 ± 99.34 $^{*,\&\&\&}$ | 69.13 | 35.51 |
| Taxol | 15 mg/kg | 102.9 ± 13.10 | 0.157 ± 0.02$^{*,\triangle\triangle\triangle,\ +++}$ | 218.5 ± 38.7$^{*,\triangle\triangle,\ +++}$ | 90.19 | 13.54 |

$^{*}P < 0.001$, compared with blank TPLE-1; $^{\Delta\Delta}P < 0.005$ and $^{\Delta\Delta\Delta}P < 0.001$, compared with TPLE-2; $^{**}P < 0.05$ and $^{***}P < 0.01$, compared with TPLE-3; $^{\&\&\&}P < 0.001$, compared with TPLE-1; $^{\triangle\triangle}P < 0.005$ and $^{\triangle\triangle\triangle}P < 0.001$, compared with TPLE-2; $^{+++}P < 0.001$, compared with TPLE-3. Data as mean ± SD ($n$ = 6).

[a] Abbreviation: TW, Tumor weight on day 9; $TV_0$ and $TV_1$, Tumor volumes on day 0 and day 9.

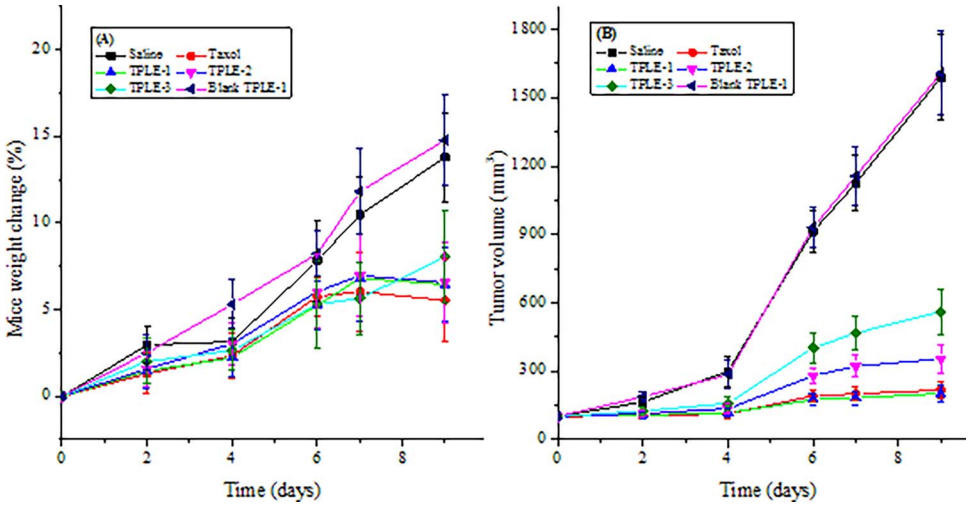


**Fig. 5.** Antitumor effects on MCF-7 tumor-bearing nude mice after intravenous administration of saline, blank TPLE-1, TPLEs and Taxol at a dosage of 15 mg/kg respectively. Tumor growth in nude mice over time (A), body weight change over time (B). Data as mean ± SD ($n$ = 6).

1 possessed lower toxicity compared to Taxol®.

## 4. Discussion and conclusion

Excessive fat infusion could cause lung, spleen, liver reticuloendothelial cell deposition, to greatly weaken the normal phagocytosis and damage the immune system for tumor patients to need long-term treatment (Cukier et al., 1999; Seidner et al., 1989). In order to prepare TPLEs with different particle size, the oil content in our previous prescription of BLE was adjusted from 20% (*w/v*) to 10% (*w/w*). The decrease of oil excipient could reduce the risk of long-term treatment. In this paper, 10% (*w/w*) injectable BLEs with particle size of 380 nm (BLE-1), 220 nm (BLE-2) and 110 nm (BLE-3) were first successfully prepared by homogenizing coarse emulsion at different homogenization cycles and pressure. Because BLEs was fully mixed by a PEG400 solution of PTX did not change original particle size and zeta potential of BLEs (Table 1), novel TPLEs with particle sizes of 110 nm (TPLE-1), 220 nm (TPLE-2) and 380 nm (TPLE-3) was expediently obtained by mixing a PEG400 solution of PTX (4 mL) with BLE-1, BLE-2 and BLE-3 (each 96 mL), respectively.

We speculated that oil phase surface area in TPLEs increased as the particle size decreased while oil content in TPLEs was all 10% (*w/w*). Since PTX was highly lipophilic and poorly soluble in water, a relative greater quantity of PTX should be tightly incorporated into oil phase of TPLEs with a smaller particle size. As a result, TPLE-1 with minimum particle size displayed distinctly higher drug-loaded, relative larger PTX distribution in oil phase and slower PTX-release compared to TPLE-2 and TPLE-3, suggesting that physical stability of TPLEs with the same drug concentration increased as the particle size decreased.

TPLE-1 exhibited stronger cytotoxicity against MCF-7 cells than TPLE-2 or TPLE-3, indicating that anticancer activity of TPLEs increased with their particle sizes decreased. Typically, drug-loaded lipid nanoparticles simultaneously entered cancer cells via two ways (Yan et al., 2010; Rejman et al., 2004; Passagne et al., 2012; Conner and Schmid, 2003). In addition, cellular uptake by tumor cell increased as particle sizes decreased and more cellular uptake results in greater tumor cell toxicity (Choi et al., 2014). However, the mechanism of TPLEs entry into tumor cells remained largely unknown. This deserved our further study.

The electrolyte in blood could cause demulsification and PTX-release after intravenous injection of emulsions to SD rats (Sakaeda and Hirano, 1998). Because TPLE-1 had better physical stability in plasma and could be phagocytosed more difficultly by reticuloendothelial cells due to its smaller particle size (Moghimi et al., 2001), it exhibited the larger plasma $AUC_{0-\infty}$ value, the longer $T_{1/2}$ and MRT, the smaller CL in plasma, implying that metabolic stability of TPLEs increased with decrease of nanoparticle size and TPLE-1 would have the stronger antitumor effect in vivo than TPLE-2 and TPLE-3.

Nanoparticles could be mainly extracted by RES organs after they are intravenously injected to nude mice bearing MCF-7 tumor. Furthermore, the smaller particle size was, the more difficult reticuloendothelial cell phagocytosis was (Moghimi et al., 2001) and the slower clearance in blood (Moreira et al., 2001) was. So, TPLE-1 showed a relative greater distribution in plasma and less share in liver/spleen/lung compared to TPLE-2 and TPLE-3. Moreover, lipid nanoparticles could selectively accumulate at tumor site by EPR effect (Lammers et al., 2012). As TPLE-1 had a relative higher distribution in plasma in form of lipid nanoparticles due to its less extraction by RES organs, slower PTX-release and smaller CL in plasma compared to TPLE-2 or TPLE-3, it could give the stronger an EPR effect. Consequently, TPLE-1 could significantly increase tumor-uptake, and exhibited most potent antitumor efficacy in vivo among TPLEs. It even had the same anticancer efficacy as Taxol®.

Lipid emulsion was firstly used as total parenteral nutrition, which was developed as a drug carrier due to its unique advantages in recent years (MacFie, 1999; Roggero et al., 2010). In addition, PEG400 was a good biocompatible polymer, which was widely used as pharmaceutical excipient with little toxicity (Larsen and Nielsen, 2002). Moreover, intravenously injection safety assessment also demonstrated that TPLE-1 had lower acute toxicity and less hemolysis and irritation response compared to Taxol®.

In short, this work demonstrates the direct correlations between particle sizes and physical stability, PTX-release, biodistribution, PK parameters, phase distribution, in vitro and in vivo antitumor efficacy for TPLEs. All results highlights the high tumor-accumulation and effectiveness, low toxicity, good safety and druggability of TPLE-1, a novel PEG400-mediated optimizational two-vial formulation of PTX-loaded lipid nanoemulsion with particle size of 110 nm, as a promising candidate drug in clinical application for the cancer therapy.

## Acknowledgement

This work was supported by the Nano Special Program Project of Science and Technology Commission of Shanghai, China (Grant nos. 0952nm03000 and 12nm0501000).

## Appendix A. Supplementary data

Supplementary data associated with this article can be found, in the online version, at https://doi.org/10.1016/j.ijpharm.2017.10.005.

## References


Akkar, A., Müller, R.H., 2003a. Formulation of intravenous carbamazepine emulsions by SolEmuls technology. Eur. J. Pharm. Biopharm. 55, 305–312.

Akkar, A., Müller, R.H., 2003b. Intravenous itraconazole emulsions produced by SolEmuls technology. Eur. J. Pharm. Biopharm. 56, 29–36.

Akkar, A., Namsolleck, P., Blaut, M., Müller, R.H., 2004. Solubilizing poorly soluble antimycotic agents by emulsification via a solvent-free process. AAPS PharmSciTech 5, 1–6.

Alexis, F., Pridgen, E.M., Langer, R., Farokhzad, O.C., 2010. Nanoparticle technologies for cancer therapy. Handb. Exp. Pharmacol. 197, 55–86.

Benita, S., Levy, M.Y., 1993. Submicron emulsions as colloidal drug carriers for intravenous administration: comprehensive physicochemical characterization. J. Pharm. Sci. 82, 1069–1079.

Choi, J.-S., Cao, J., Naeem, M., Noh, J., Hasan, N., Choi, H.-K., Yoo, J.-W., 2014. Size-controlled biodegradable nanoparticles: preparation and size-dependent cellular uptake and tumor cell growth inhibition. Colloids Surf. B 122, 545–551.

Conner, S.D., Schmid, S.L., 2003. Regulated portals of entry into the cell. Nature 422, 37–44.

Cukier, C., Waitzberg, D.L., Logullo, A.F., Bacchi, C.E., Travassos, V.H., Torrinhas, R.S.M., Soares, S.R.C., Saldiva, P.H., Oliveira, T.S., Heymsfield, S., 1999. Lipid and lipid-free total parenteral nutrition: differential effects on macrophage phagocytosis in rats. Nutrition 15, 885–889.

Fukui, H., Koike, T., Saheki, A., Sonoke, S., Seki, J., 2003. A novel delivery system for amphotericin B with lipid nano-sphere (LNS). Int. J. Pharm. 265, 37–45.

Ganta, S., Paxton, J.W., Baguley, B.C., Garg, S., 2008. Pharmacokinetics and pharmacodynamics of chlorambucil delivered in parenteral emulsion. Int. J. Pharm. 360, 115–121.

Gao, L., Liu, G., Kang, J., Niu, M., Wang, Z., Wang, H., Ma, J., Wang, X., 2013. Paclitaxel nanosuspensions coated with P-gp inhibitory surfactants: i. Acute toxicity and pharmacokinetics studies. Colloids Surf. B 111, 277–281.

Hippalgaonkar, K., Majumdar, S., Kansara, V., 2010. Injectable lipid emulsions-advancements, opportunities and challenges. AAPS PharmSciTech 11, 1526–1540.

Jeppsson, R., Ljungberg, S., 1975. Anticonvulsant activity in mice of diazepam in an emulsion formulation of intravenous administration. Acta Pharmacol. Toxicol. 36, 312–320.

Jing, X., Deng, L., Gao, B., Xiao, L., Zhang, Y., Ke, X., Lian, J., Zhao, Q., Ma, L., Yao, J., Chen, J., 2014. A novel polyethylene glycol mediated lipid nanoemulsion as drug delivery carrier for paclitaxel. Nanomed.-Nanotechnol 10, 371–380.

Keck, C.M., Müller, R.H., 2006. Drug nanocrystals of poorly soluble drugs produced by high pressure homogenisation. Eur. J. Pharm. Biopharm. 62, 3–16.

Kelmann, R.G., Kuminek, G., Teixeira, H.F., Koester, L.S., 2008. Preliminary study on the development of nanoemulsions for carbamazepine intravenous delivery: an investigation of drug polymorphic transition. Drug Dev. Ind. Pharm. 34, 53–58.

Kesisoglou, F., Panmai, S., Wu, Y., 2007. Nanosizing–oral formulation development and biopharmaceutical evaluation. Adv. Drug Deliv. Rev. 59, 631–644.

Krause, K.P., Kayser, O., Mader, K., Gust, R., Müller, R.H., 2000. Heavy metal contamination of nanosuspensions produced by high-pressure homogenisation. Int. J. Pharm. 196, 169–172.

Lammers, T., Kiessling, F., Hennink, W.E., Storm, G., 2012. Drug targeting to tumors: principles, pitfalls and (pre-) clinical progress. J. Control. Release 161, 175–187.

Larsen, S.T., Nielsen, G.D., 2002. Thygesen P: Investigation of the adjuvant effect of polyethylene glycol (PEG) 400 in BALB/c mice. Int. J. Pharm. 231, 51–55.

Lee, J.Y., Bae, K.H., Kim, J.S., Nam, Y.S., Park, T.G., 2011. Intracellular delivery of paclitaxel using oil-free, shell cross-linked HSA–multi-armed PEG nanocapsules. Biomaterials 32, 8635–8644.

Li, X., Choi, J.S., 2007. Effect of genistein on the pharmacokinetics of paclitaxel administered orally or intravenously in rats. Int. J. Pharm. 337, 188–193.

Lipinski, C.A., 2000. Drug-like properties and the causes of poor solubility and poor permeability. J. Pharmacol. Toxicol. Methods 44, 235–249.

Müller, R.H., Schmidt, S., Buttle, I., Akkar, A., Schmitt, J., Bromer, S., 2004. SolEmuls-novel technology for the formulation of i.v. emulsions with poorly soluble drugs. Int. J. Pharm. 269, 293–302.

Ma, P., Rahima Benhabbour, S., Feng, L., Mumper, R.J., 2013. 2'-Behenoyl-paclitaxel conjugate containing lipid nanoparticles for the treatment of metastatic breast cancer. Cancer Lett. 334, 253–262.

MacFie, J., 1999. The development of fat emulsions. Nutrition 15, 643–645.

Mao, J., Song, B., Shi, Y., Wang, B., Fan, S., Yu, X., Tang, J., Li, L., 2013. ShRNA targeting Notch1 sensitizes breast cancer stem cell to paclitaxel. Int. J. Biochem. Cell Biol. 45, 1064–1073.

Mishra, P.R., Al Shaal, L., Müller, R.H., Keck, C.M., 2009. Production and characterization of Hesperetin nanosuspensions for dermal delivery. Int. J. Pharm. 371, 182–189.

Moghimi, S.M., Hunter, A.C., Murray, J.C., 2001. Long-circulating and target-specific nanoparticles: theory to practice. Pharmacol. Rev. 53, 283–318.

Moreira, J.N., Gaspar, R., Allen, T.M., 2001. Targeting Stealth liposomes in a murine model of human small cell lung cancer. Biochim. Biophys. Acta 1515, 167–176.

Passagne, I., Morille, M., Rousset, M., Pujalte, I., L'Azou, B., 2012. Implication of oxidative stress in size-dependent toxicity of silica nanoparticles in kidney cells. Toxicology 299, 112–124.

Rejman, J., Oberle, V., Zuhorn, I.S., Hoekstra, D., 2004. Size-dependent internalization of particles via the pathways of clathrin- and caveolae-mediated endocytosis. Biochem. J. 377, 159–169.

Roggero, P., Mosca, F., Gianni, M.L., Orsi, A., Amato, O., Migliorisi, E., Longini, M., Buonocore, G., 2010. F2-isoprostanes and total radical-trapping antioxidant potential in preterm infants receiving parenteral lipid emulsions. Nutrition 26, 551–555.

Sakaeda, T., Hirano, K., 1998. Effect of composition on biological fate of oil particles after intravenous injection of O/W lipid emulsions. J. Drug Target. 6, 273–284.

Sarker, D.K., 2005. Engineering of nanoemulsions for drug delivery. Curr. Drug Deliv. 2, 297–310.

Seidner, D.L., Mascioli, E.A., Istfan, N.W., Porter, K.A., Selleck, K., Blackburn, G.L., Bistrian, B.R., 1989. Effects of long-chain triglyceride emulsions on reticuloendothelial system function in humans. J. Parenteral Enteral Nutr. 13, 614–619.

Seki, J., Sonoke, S., Saheki, A., Fukui, H., Sasaki, H., Mayumi, T., 2004. A nanometer lipid emulsion, lipid nano-sphere (LNS), as a parenteral drug carrier for passive drug targeting. Int. J. Pharm. 273, 75–83.

Shaikh, J., Ankola, D.D., Beniwal, V., Singh, D., Kumar, M.N., 2009. Nanoparticle encapsulation improves oral bioavailability of curcumin by at least 9-fold when compared to curcumin administered with piperine as absorption enhancer. Eur. J. Pharm. Sci. 37, 223–230.

Sila-on, W., Vardhanabhuti, N., Ongpipattanakul, B., Kulvanich, P., 2008. Influence of incorporation methods on partitioning behavior of lipophilic drugs into various phases of a parenteral lipid emulsion. AAPS PharmSciTech 9, 684–692.

Suttmann, H., Doenicke, A., Kugler, J., Laub, M., 1989. A new formulation of etomidate in lipid emulsion–bioavailability and venous provocation. Anaesthesist 38, 421–423.

Takegami, S., Kitamura, K., Kawada, H., Matsumoto, Y., Kitade, T., Ishida, H., Nagata, C., 2008. Preparation and characterization of a new lipid nano-emulsion containing two cosurfactants: sodium palmitate for droplet size reduction and sucrose palmitate for stability enhancement. Chem. Pharm. Bull. 56, 1097–1102.

Takino, T., Konishi, K., Takakura, Y., Hashida, M., 1994. Long circulating emulsion carrier systems for highly lipophilic drugs. Biol. Pharm. Bull. 17, 121–125.

Tamilvanan, S., 2004. Oil-in-water lipid emulsions: implications for parenteral and ocular delivering systems. Prog. Lipid Res. 43, 489–533.

Yan, F., Zhang, C., Zheng, Y., Mei, L., Tang, L., Song, C., Sun, H., Huang, L., 2010. The effect of poloxamer 188 on nanoparticle morphology, size, cancer cell uptake, and cytotoxicity. Nanomed.-Nanotechnol 6, 170–178.

Yao, H.J., Ju, R.J., Wang, X.X., Zhang, Y., Li, R.J., Yu, Y., Zhang, L., Lu, W.L., 2011. The antitumor efficacy of functional paclitaxel nanomicelles in treating resistant breast cancers by oral delivery. Biomaterials 32, 3285–3302.

Zhang, C., Qu, G., Sun, Y., Wu, X., Yao, Z., Guo, Q., Ding, Q., Yuan, S., Shen, Z., Ping, Q., Zhou, H., 2008. Pharmacokinetics, biodistribution, efficacy and safety of N-octyl-O-sulfate chitosan micelles loaded with paclitaxel. Biomaterials 29, 1233–1241.

Zhu, H., Liu, Z., Tang, L., Liu, J., Zhou, M., Xie, F., Wang, Z., Wang, Y., Shen, S., Hu, L., Yu, L., 2012. Reversal of P-gp and MRP1-mediated multidrug resistance by H6 a gypenoside aglycon from Gynostemma pentaphyllum, in vincristine-resistant human oral cancer (KB/VCR) cells. Eur. J. Pharmacol. 696, 43–53.

von Dardel, O., Mebius, C., Mossberg, T., Svensson, B., 1983. Fat emulsion as a vehicle for diazepam. A study of 9492 patients. Br. J. Anaesth. 55, 41–47.